Supplementary Material for

Satellite-Detected Nitrogen Oxides Emission Changes from Power Plant Dynamics in North China

Chenghao Xu[1], Jintai Lin[1,2,*], Sijie Wang[1], Hao Kong[1], Yuhang Zhang[1], Yang Yun[1], Fangxuan Ren[1], Mengying Wang[1], Wanshan Tan[1], Jianxiao Wang[3,4], Lei Bai[5] and Jian Gao[6]

[1] Laboratory for Climate and Ocean-Atmosphere Studies, Department of Atmospheric and Oceanic Sciences, School of Physics, Peking University, Beijing 100871, People's Republic of China

[2] Institute of Carbon Neutrality, Peking University, Beijing 100871, People's Republic of China

[3] National Engineering Laboratory for Big Data Analysis and Applications, Peking University, Beijing 100871, People's Republic of China

[4] Peking University Ordos Research Institute of Energy, Ordos 017000, People's Republic of China

[5] Shanghai Artificial Intelligence Laboratory, Shanghai 200232, People's Republic of China

[6] State Key Laboratory of Environmental Criteria and Risk Assessment, Chinese Research Academy of Environmental Sciences, Beijing 100012, People's Republic of China

*Author to whom any correspondence should be addressed.

E-mail: linjt@pku.edu.cn

Received xxxxxx

Accepted for publication xxxxxx

Published xxxxxx

Section S1. Temporal Representativeness of TROPOMI overpass timing.

The use of TROPOMI overpass data (~13:30 local time) for PHLET-based emission inversion rests on the following implicit assumptions: (i) power plant emissions at overpass time are representative of summer mean emission levels; (ii) growing solar penetration over 2018–2024 does not significantly influence the representativeness. We now explicitly enumerate and assess each assumption in the revised Discussion.

(1) Differential Applicability by Plant Category

Assumption validity differs systematically across plant categories. For large, newly built ULE plants (most > 500 MW)—predominantly supercritical and ultra-supercritical units—baseload operation is the technical and economic norm. These units are grid-stabilising baseload assets, and assumption (i) holds to a good approximation.

For retired plants, which are predominantly small, subcritical legacy units (most < 200 MW, concentrated in Hebei Province), load-following behaviour prior to retirement is more plausible. We assess the potential bias under two bounding scenarios:

Conservative scenario (no midday load-following): Retired legacy units operated at constant minimum technical output at overpass time. According to multiple official and peer-reviewed sources, unmodified legacy units in China have minimum technical output ratios of approximately 50% of rated capacity under normal operation(National Development and Reform Commission, 2018, 2021; Xu et al., 2024). Under this scenario, TROPOMI captures emissions at 50–60% load—somewhat below typical daytime operation—and would slightly underestimate pre-retirement emissions.

Extreme scenario (maximum midday peaking): Retired legacy units ramped from minimum technical output (~50% rated capacity) to full rated capacity exactly at the TROPOMI overpass. In this case, TROPOMI captures emissions at full-load operation—the absolute upper bound on pre-retirement emission levels.

Assessment of net impact: Even under the extreme scenario, the directional conclusion remains robust. The retired legacy units have median installed capacities several times smaller than the newly built ULE plants. More importantly, the emission factors of uncontrolled legacy units are at least one order of magnitude higher per unit of capacity than those of ULE-equipped new plants. The key comparison in our analysis is between the emission reduction observed at retired legacy plant grid cells and the emission increase observed at newly built ULE plant grid cells (non-industry-influenced; Figure 4a and 4c). From our satellite-derived data, the mean emission reduction at retired plant grid cells is 1.97 kg km^{-2} h^{-1}, which already exceeds the mean emission increase at newly built plant grid cells (0.76 kg km^{-2} h^{-1}) by a factor of approximately 2.6. Now consider the most extreme scenario: if all retired legacy units were operating at full rated capacity precisely at the TROPOMI overpass—rather than at the minimum technical output of ~50% rated capacity assumed in the conservative scenario—the true pre-retirement emissions would be at most a factor of 2 times higher than those captured under constant minimum-load operation. This would imply an upper-bound correction of approximately ×2 on the observed pre-retirement emission level. Even after halving the observed pre-retirement emissions (i.e.,

applying the most aggressive possible downward correction to account for load-following behaviour), the corrected emission reduction at retired plant grid cells (approximately $0.5 \times 1.97 \approx 0.99$ kg km^{-2} h^{-1}) remains comparable to, and in many individual cases still exceeds, the mean post-commissioning emission increase at newly built ULE plants (0.76 kg km^{-2} h^{-1}). Therefore, the conclusion that pre-retirement emissions from legacy plants exceed post-commissioning emissions from new ULE plants holds under both the conservative and extreme scenarios. The uncertainty introduced by intraday load variation is bounded and does not alter the qualitative conclusions.

(2) Solar Generation

We acknowledge that midday solar displacement of thermal generation constitutes a legitimate concern, particularly given the rapid capacity expansion over the study period. We now provide a semi-quantitative assessment.

Based on data from the National Bureau of Statistics (Obtained from https://data.stats.gov.cn/dg/website/page.html#/pc/national/fsMonthData, Last access: Jun 19, 2026), summertime solar generation as a fraction of total thermal generation in North China grew from 1.6% in summer 2018 to 5.8% in summer 2024. Solar power exhibits a strongly peaked diurnal profile: midday output (approximately 11:00–14:00 LST) is typically about 3 times the all-day average based on documented solar irradiance climatology over China (Fan et al., 2018; Jiang et al., 2020). Applying the average situation (3×), the instantaneous ratio of solar to thermal power generation at the TROPOMI overpass in summer 2024 is estimated at:

$$\text{Ratio} \approx 5.8\% \times 3 \div (100\% + 5.8\% - 5.8\% \times 3) = 19.7\%$$

This represents an upper-bound suppression of thermal output at overpass time of $\leq$ ~20% in 2024, with substantially smaller effects in earlier years (~5% in summer 2018), we consider this uncertainty range is acceptable. Besides, solar-induced thermal suppression affects both newly built and retired plant grid cells without introducing a systematic directional bias between the two categories, and the uncertainty therefore does not compromise the directional conclusions of the study.

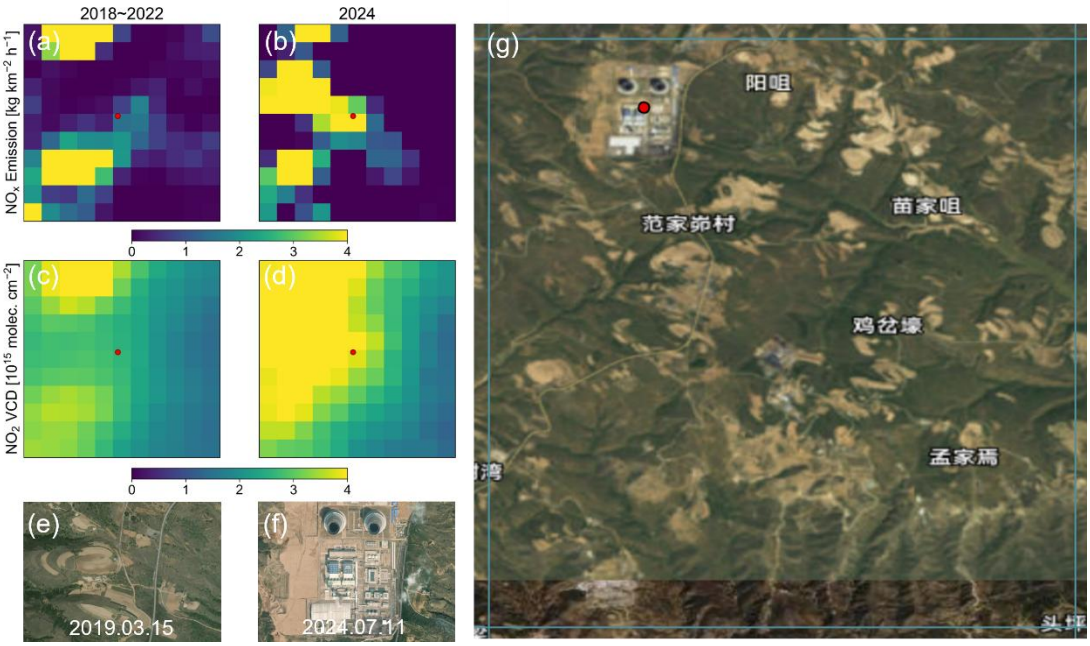


Figure S1. Detailed information on a newly built power plant (No. 43). For this plant, Unit I started operation in July 2023, and Unit II started operation in November 2023. (a, b) Distribution of averaged summer NO_x emissions at 0.55° × 0.55° (11 × 11 grid cells) around the power plant before and after build-up. (c, d) Distribution of averaged summer NO_2 VCDs around the power plant before and after build-up. (e, f) Satellite imagery before and after the power plant build-up. (g) Satellite imagery of the PHLET grid cell (0.05° × 0.05°) containing No. 43 power plant (red dot).

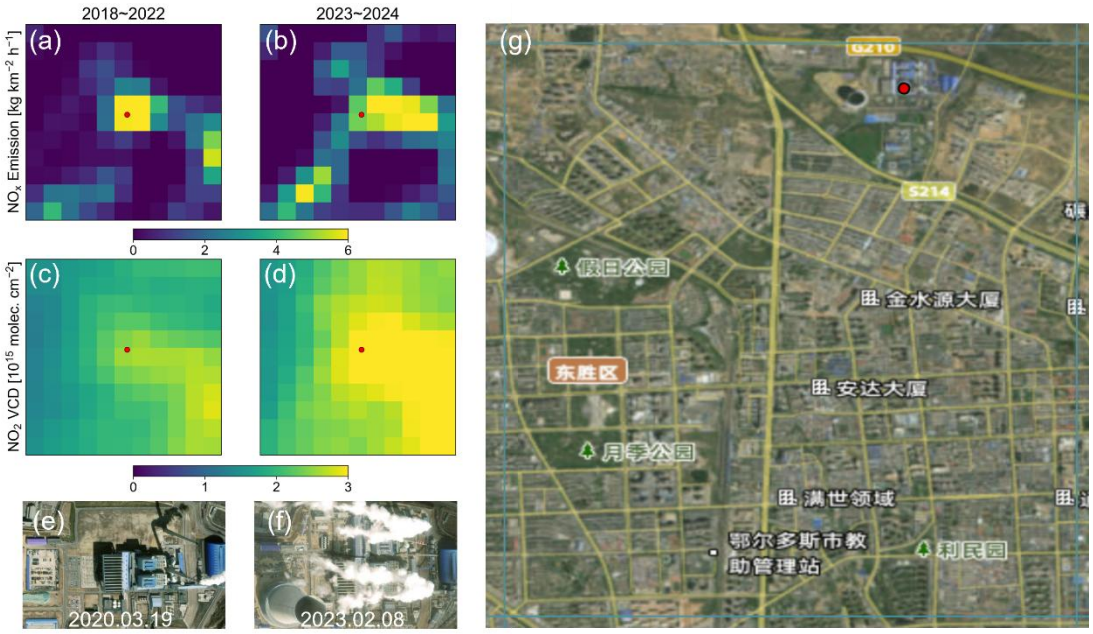


Figure S2. Detailed information on a newly built power plant (No. 53). For this plant, Phase I power generation units were operational during the study period, and Phase II units started operation in January 2023. (a, b) Distribution of averaged summer NO_x emissions at 0.55° × 0.55° (11 × 11 grid cells) around the power plant before and after build-up. (c, d) Distribution of averaged summer NO_2 VCDs around the power plant before and after build-up. (e, f) Satellite imagery before and after the power plant build-up. (g) Satellite imagery of the PHLET grid cell (0.05° × 0.05°) containing No. 53 power plant (red dot).

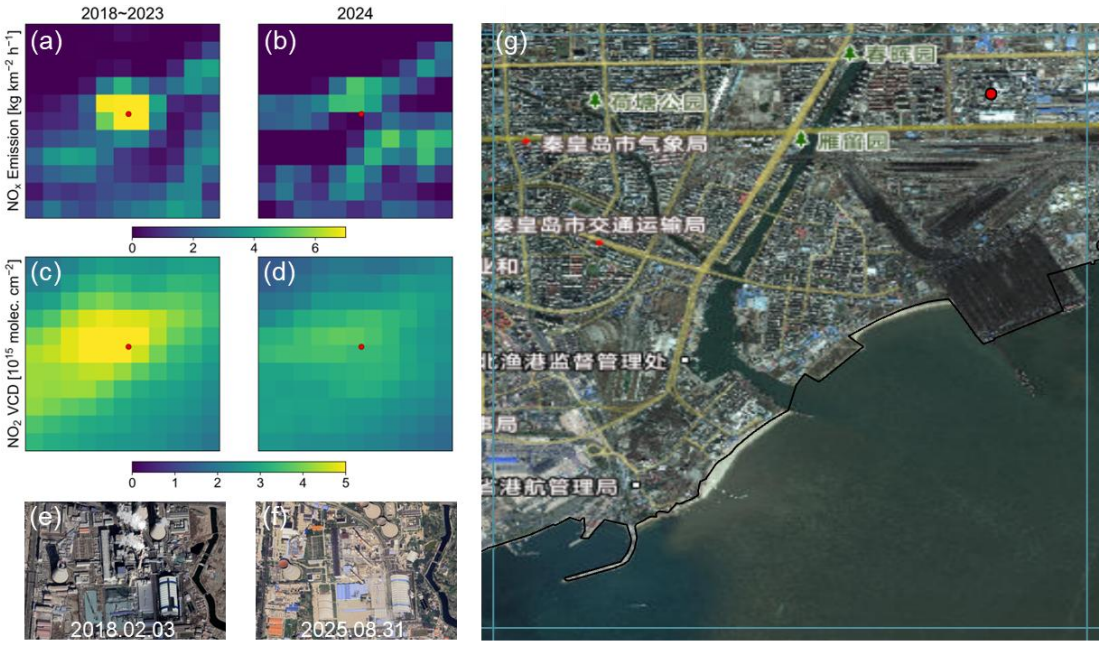


Figure S3. Detailed information on a retired power plant (No. 104). This plant was retired in 2024. (a, b) Distribution of averaged summer NO_x emissions at 0.55° × 0.55° (11 × 11 grid cells) around the power plant before and after retirement. (c, d) Distribution of averaged summer NO_2 VCDs around the power plant before and after retirement. (e, f) Satellite imagery before and after power plant retirement. (g) Satellite imagery of the PHLET grid cell (0.05° × 0.05°) containing No. 104 power plant (red dot).

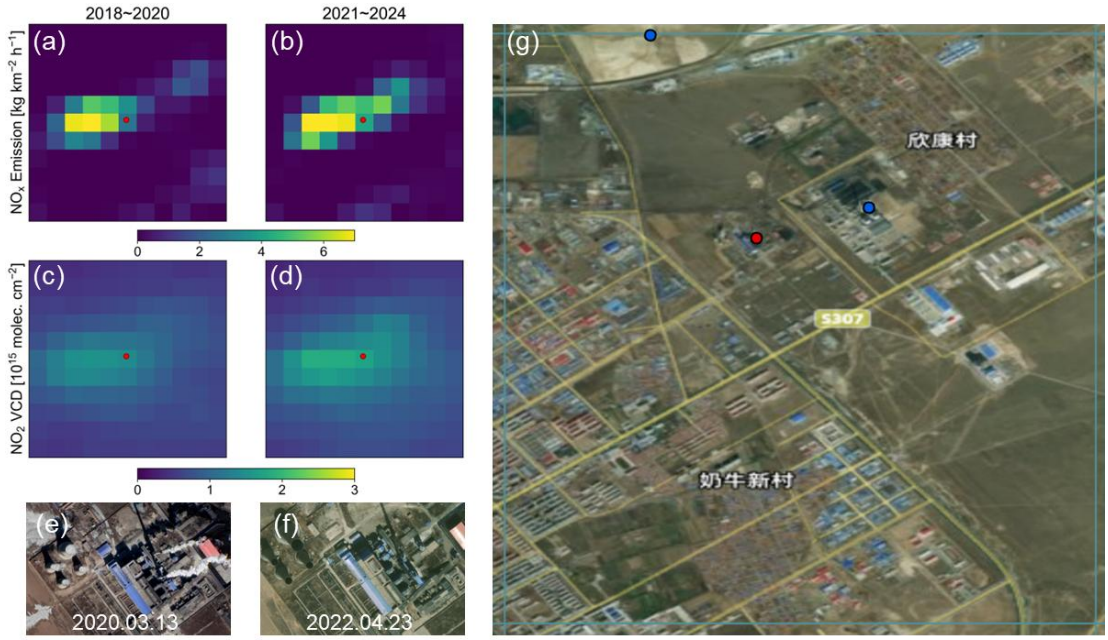


Figure S4. Detailed information on a retired power plant (No. 94). This plant was retired in 2021. (a, b) Distribution of averaged summer NO_x emissions at 0.55° × 0.55° (11 × 11 grid cells) around the power plant before and after retirement. (c, d) Distribution of averaged summer NO_2 VCDs around the power plant before and after retirement. (e, f) Satellite imagery before and after power plant retirement. (g) Satellite imagery of the PHLET grid cell (0.05° × 0.05°) containing No. 94 power plant (red dot). Two other power plants were newly built in this grid cell (No. 30 and No. 48, blue dots).

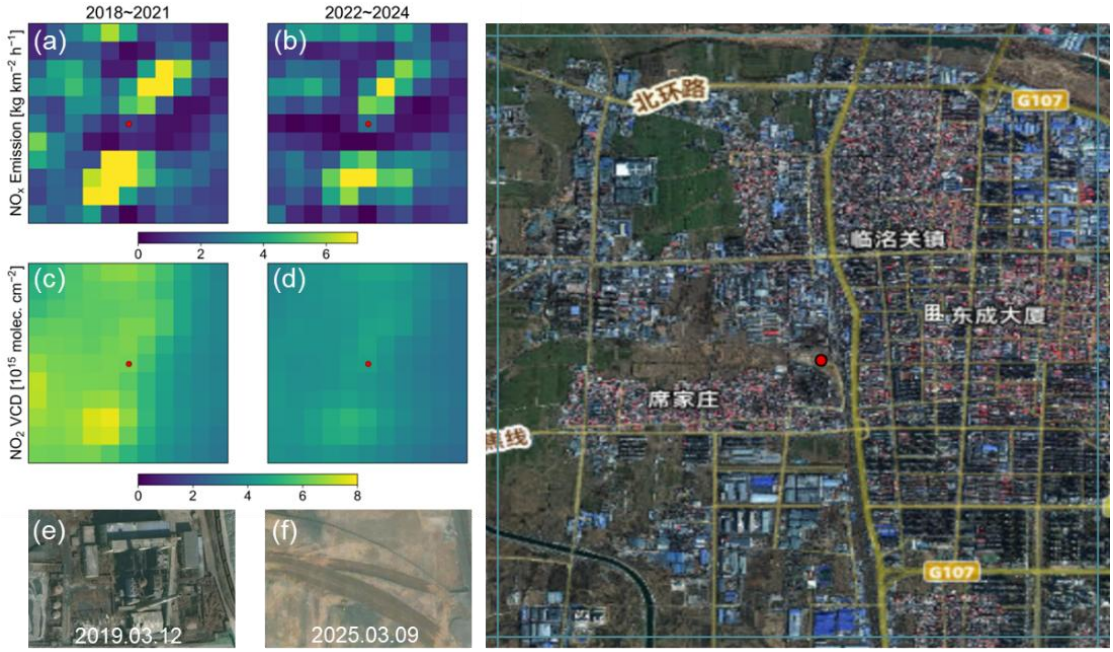


Figure S5. Detailed information on a retired power plant (No. 63). This plant was retired in 2022, but its emission signal could be influenced by transportation. (a, b) Distribution of averaged summer NO_x emissions at 0.55° × 0.55° (11 × 11 grid cells) around the power plant before and after retirement. (c, d) Distribution of averaged summer NO_2 VCDs around the power plant before and after retirement. (e, f) Satellite imagery before and after power plant retirement. (g) Satellite imagery of the PHLET grid cell (0.05° × 0.05°) containing No. 63 power plant (red dot).